JOURNAL OF GUIDANCE, CONTROL, AND DYNAMICS
Vol. 34, No. 2, March–April 2011

Engagement Tactics for Two Missiles Against an Optimally Maneuvering Aircraft

Fumiaki Imado*
Shinshu University, Nagano 380-8553, Japan
and
Takeshi Kuroda†
Mitsubishi Electric Corporation, Hyogo 661-8661, Japan

DOI: 10.2514/1.49079

The engagement tactics for two missiles to attack an aircraft are studied. A tail chase scenario between two aircraft is assumed where the attacker tries to kill the evader with two missiles, while the evader employs optimal maneuvers for avoiding two missiles. The algorithm to solve this optimal control problem is first developed. For the aircraft, in order to simultaneously maximize the miss distances against two missiles, a special type of performance index is introduced and the problems are solved by the solver based on the steepest ascent method. The result shows that the aircraft optimal maneuvers are divided into three patterns. Next, the optimal timing for the attacker to launch the two missiles, in order to minimize both miss distances against the aircraft is studied. The effect of their taking trajectory shaping is also studied.

Nomenclature

A	=	aircraft
a	=	lateral acceleration
a_c	=	missile lateral acceleration command signal
C_D, C_L	=	drag and lift coefficients, respectively
C_{D0}	=	zero-lift drag coefficient
D	=	drag
$\boldsymbol{f}$	=	state derivative vector
H	=	Hamiltonian function
h	=	altitude
I_{sp}	=	specific impulse
J	=	performance index
k	=	induced drag of aircraft
k_1, k_2, k_m	=	drag coefficients of missile
L	=	lift
M	=	missile
m	=	mass
N_e	=	missile navigation gain
n	=	power of penalty function
p	=	penalty function for the first missile
r	=	slant range between missile and aircraft
r_{12}	=	initial distance between two missiles
r_{1a}	=	reference value of the slant range between the first missile and aircraft
r_{1f}, r_{2f}	=	closest ranges (miss distances) between the aircraft and the first and second missiles, respectively
r_m	=	the mean miss distance between two missiles, $(r_{1f}.r_{2f})^{\frac{1}{2}}$
S	=	reference area
T	=	thrust
t	=	time
t_e	=	sustainer burning time
t_f	=	interception time
t_{w1}, t_{w2}	=	start time and end time of window function
$\boldsymbol{u}$	=	control vector
v	=	velocity
v_c	=	closing velocity
w	=	window function
x, y	=	longitudinal and lateral coordinates
$\boldsymbol{x}$	=	state vector
α, α_0	=	angle-of-attack and zero-lift angle, respectively
$\boldsymbol{\lambda}$	=	adjoint vector
ρ	=	air density
σ, ψ	=	line-of-sight and azimuth angles, respectively
τ	=	missile time constant
ϕ	=	performance index for minimizing both miss distances
Ω	=	stopping condition
$\boldsymbol{\psi}$	=	terminal constraints
$(\dot{\cdot})$	=	time derivative

Subscripts

a	=	aircraft
c	=	command signal
i	=	ith missile
m	=	missile
max, min	=	maximum and minimum values, respectively

I. Introduction

A TYPICAL fighter is provided with two short range missiles and two medium range missiles as well as other weapons. In a one-on-one engagement, and supposing one has achieved an advantageous position to another and has caught the enemy in his lethal cone, he has to employ his missiles most effectively. Many studies have appeared about optimal missile avoidance by an aircraft [1–20], however, only a few papers have treated avoiding multiple missiles [12,18]. The reason for this could be that it is difficult for an aircraft to avoid even one missile, therefore avoiding two missiles is not realistic. However, as stated, in actual situations an aircraft can use two short range missiles or medium range missiles depending on the relative distance. Also the development of unmanned aerial vehicles (UAV) has drastically changed the situation. The miss distance (MD) is approximately proportional to the square of the aircraft maximum lateral acceleration$a_{a\,\max}$, which is limited by the endurance of the pilot in a manned aircraft. On the other hand, since in UAVs this limit is not applicable and a larger lateral acceleration can be produced,

Received 25 January 2010; revision received 14 May 2010; accepted for publication 2 November 2010.

*Professor, Department of Mechanical Systems Engineering; imadofu@shinshu-u.ac.jp. Senior Member AIAA.

†Senior Engineer, Advanced Technology Research and Development Center; Kuroda.Takeshi@dy.MitsubishiElectric.co.jp.

they may avoid even two missiles simultaneously. Therefore, studying the features of such maneuvers and the counter strategy of the attacker will be useful for engineers of both missiles and aircraft as well as aircraft pilots. The former study [12] showed the geometric analysis between two missiles and an aircraft. The study conducted a massive number of simulations for randomly maneuvering aircraft and tried to find the optimal relative geometry of vehicles. The other study [18] succeeded in finding two typical optimal aircraft maneuvers against two proportional navigation (PN) [21,22] missiles. The optimal controls of the aircraft were solved by the STP-CODE (STeePest ascent CODE), which is a general optimization program developed by the authors based on the steepest ascent method [23,24]. As the algorithm has been improved since then, currently the solutions to avoid two missiles can be obtained under any initial relative geometries. A recent study of the authors found the aircraft optimal maneuvers are divided into three patterns depending on the relative geometry. In Sec. II, equations for nonlinear optimal control problems employed in the steepest ascent method are briefly shown. In Sec. III, the mathematical model and the derivation of the optimal aircraft maneuver against two PN missiles is explained. A typical medium range air-to-air missile, and a pure tail chase scenario are assumed here. In Sec. IV, two missiles' optimal geometry, in other words, the optimal launching times of two missiles against an optimally-maneuvering aircraft are studied. To attack the aircraft from different directions, the trajectory shaping of the two missiles are also considered and the effect is studied in Sec. V. These results are discussed in Sec. VI, and summarized in the Conclusion.

II. Equations for Nonlinear Optimal Control Problems

Before this study, an algorithm to obtain the aircraft optimal maneuver which simultaneously maximizes the MDs against two missiles had to be developed. The solver developed by the authors is called the STP-CODE which is based on the steepest ascent method. In this section, equations for nonlinear optimal control problems employed in the steepest ascent method are briefly shown. A general nonlinear optimal control problem is stated as follows:

Find optimal control $\boldsymbol{u}(t)$, $(0 \le t \le t_f)$ to maximize the following performance index (Mayer-type is assumed) J (for minimizing, change the sign of ϕ):

$$J = \phi\lfloor \boldsymbol{x}(t_f), t_f \rfloor \tag{1}$$

subject to the following equations:

$$\dot{\boldsymbol{x}} = \boldsymbol{f}(\boldsymbol{x}, \boldsymbol{u}, t) \tag{2}$$

$$\boldsymbol{x}\,(t_0) = \boldsymbol{x}_0\text{:specified} \tag{3}$$

with terminal constraints

$$\boldsymbol{\psi}\,[\boldsymbol{x}(t_f), t_f] = 0 \tag{4}$$

where $\boldsymbol{x}(t)$ is an n-dimensional state vector, $\boldsymbol{u}(t)$ is an m-dimensional control vector, and ψ is a q-dimensional constraint vector. The Hamiltonian H is

$$H = \lambda^T \boldsymbol{f} \tag{5}$$

The adjoint equations and boundary conditions are given by

$$\dot{\boldsymbol{\lambda}} = -\frac{\partial H}{\partial \boldsymbol{x}} = -\boldsymbol{\lambda}^T \frac{\partial \boldsymbol{f}}{\partial \boldsymbol{x}} \tag{6}$$

$$\boldsymbol{\lambda}\,(t_f) = -\left(\frac{\partial \Phi}{\partial \boldsymbol{x}}\right)^T_{t=t_f} \tag{7}$$

where

$$\Phi = \phi + \boldsymbol{\nu}^T \boldsymbol{\psi} \tag{8}$$

where the unknown multiplier $\boldsymbol{\nu}$ is determined through the terminal constraints Eq. (4). Equations (1–8) are called Euler–Lagrange equations. For an extremum, the differential change of the performance index δJ must be zero for arbitrary differential change of $\boldsymbol{u}(t)$: $\delta \boldsymbol{u}(t)$, that is, the following condition of optimality has to be satisfied:

$$\frac{\partial H}{\partial \boldsymbol{u}} = 0 \qquad (t_0 \le t \le t_f) \tag{9}$$

If there are constraints on the values of $\boldsymbol{u}(t)$, e.g. $u_i \le u_{i\,\max}$, then in Eq. (9) u_i has to satisfy

$$\frac{\partial H}{\partial u_i} = 0 \quad \text{or} \quad u_i = u_{i\,\max} \qquad (t_0 \le t \le t_f) \tag{10}$$

The transversality condition at the final time t_f is

$$H(t_f) = -\left(\frac{\partial \Phi}{\partial t}\right)_{t=t_f} \tag{11}$$

In the steepest ascent algorithm (STP) in [24], corresponding to Eq. (11), the stopping condition which determines the final time is defined:

$$\Omega[\boldsymbol{x}(t_f), t_f] = 0 \tag{12}$$

In Eq. (12), Ω can be selected from any arbitrary components of $\boldsymbol{\psi}$ in Eq. (4), however, it must clearly determine the final time t_f. The constraints Eq. (4) can be introduced by penalty functions into the performance index Eq. (1) instead of the method appearing in [24]. In this paper, a special penalty function is introduced in Sec. III.

III. Derivation of an Aircraft vs Two-Missiles Problem

If the aircraft has not enough time to fly away from the attacker, the next tactic is to provide for the missiles to come. In this case the aircraft should take a pure tail chase geometry to provide for any missile attack because then it can implement optimal evasive maneuvers for any symmetrical missile attacks. Figure 1 shows the relative geometry of a pursuer (missile) and the evader (aircraft), and related symbols. As the purpose of this study is to know the optimal distances between the two missiles and the aircraft, the motions are constrained in a horizontal plane. The following equations and formulation are used for the calculation of the optimal aircraft control. Both vehicles are modeled as point masses, where suffixes "a" and "m_i" express aircraft and ith missile. The aircraft is assumed to have perfect knowledge of all vehicle dynamics as well as the guidance strategy of the missiles:

$$\dot{v}_a = \frac{T_a \cos\alpha - D}{m_a} \tag{13}$$

$$\dot{\psi}_a = \frac{L + T_a \sin\alpha}{m_a v_a} \tag{14}$$

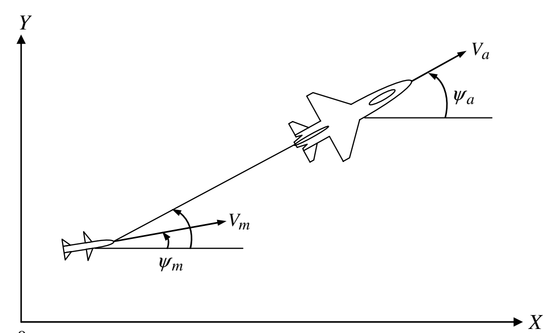

Fig. 1 Vehicle geometry and symbols.

$$\dot{x}_a = v_a \cos\psi_a \tag{15}$$

$$\dot{y}_a = v_a \sin\psi_a \tag{16}$$

$$L = \frac{1}{2}\rho_a v_a^2 S_a C_L \qquad D = \frac{1}{2}\rho_a v_a^2 S_a C_D \tag{17}$$

$$C_L = C_{L\alpha}(\alpha - \alpha_0) \qquad C_D = C_{D0} + kC_L^2 \tag{18}$$

$$\rho_a = \rho_a(h_a), \qquad T_a = T_a(v_a, h_a) \tag{19}$$

A constraint is imposed on the value of the aircraft angle-of-attack α, which is treated as the aircraft control variable:

$$|\alpha| \le \alpha_{\max} \tag{20}$$

where a negative α is considered as a positive α with a bank angle of -90 deg. The missile lateral acceleration is approximated by a first-order lag to a lateral acceleration command signal a_{mic}:

$$\dot{v}_{mi} = \frac{T_{mi} - D_{mi}}{m_{mi}} \tag{21}$$

$$\dot{a}_{mi} = \frac{a_{mic} - a_{mi}}{\tau_i} \tag{22}$$

$$\dot{\psi}_{mi} = \frac{a_{mi}}{v_{mi}} \tag{23}$$

$$\dot{x}_{mi} = v_{mi}\cos\psi_{mi} \tag{24}$$

$$\dot{y}_{mi} = v_{mi}\sin\psi_{mi} \tag{25}$$

where

$$D_{mi} = k_{1i}v_{mi}^2 + k_{2i}\left(\frac{a_{mi}}{v_{mi}}\right)^2 \tag{26}$$

$$k_{1i} = \frac{1}{2}\rho_{mi}S_{mi}C_{D0mi} \quad k_{2i} = \frac{2k_{mi}m_{mi}^2}{\rho_{mi}S_{mi}} \tag{27}$$

$$T_{mi}(t) = \begin{cases} T_{mi} & \text{for } 0 \le t \le t_{ei} \\ 0 & \text{for } t_{ei} < t \end{cases} \tag{28}$$

For a PN missile with signal saturation taken into consideration, a_{mic} is given by

$$a_{mic} = \begin{cases} N_{ei}v_{ci}\dot{\sigma}_i & \text{for } |a_{mic}| \le a_{mic\max} \\ a_{mic\max}\,\text{sign}(a_{ci}) & \text{for } |a_{mic}| > a_{mic\max} \end{cases} \tag{29}$$

where N_{ei} is the effective navigation ratio, v_{ci} the closing velocity, and $\dot{\sigma}_i$ the line-of-sight turning rate given by

$$v_{ci} = -\dot{r}_i \tag{30}$$

$$\dot{\sigma}_i = \frac{(y_a - y_{mi})(\dot{x}_a - \dot{x}_{mi}) - (\dot{y}_a - \dot{y}_{mi})(x_a - x_{mi})}{r_i^2} \tag{31}$$

where r_i is the slant range:

$$r_i = [(x_a - x_{mi})^2 + (y_a - y_{mi})^2]^{\frac{1}{2}} \tag{32}$$

To maximize the MD for the first missile, the following state and window function are introduced:

$$\dot{p} = w(t)\left(\frac{r_{1a}}{r_1}\right)^n \tag{33}$$

$$w(t) = \begin{cases} 1.0 & \text{for } t_{w1} \le t \le t_{w2} \\ 0 & \text{for } 0 \le t < t_{w1}, t_{w2} < t \end{cases} \tag{34}$$

where t_{w1} and t_{w2} are selected to include the time of the closest approach point (CAP) for the first missile, and r_{1a} is a constant. The following performance index is introduced:

$$\phi = \{k_r r_2^2 - k_{rf}(r_2 - r_{2f})^2 - k_p p\}_{t=t_f} \tag{35}$$

where the terminal time t_f is obtained from the following stopping condition:

$$\Omega \equiv \dot{r}_2 = 0 \tag{36}$$

which means the time of the CAP with the second missile. The meaning of Eqs. (33–35) is explained later in detail. The problem is to find the control history of $\alpha(t)$ which maximizes ϕ of Eq. (35) under differential Eqs. (13–16) and (21–25), $(i = 1, 2)$, and (33) with a constraint of Eq. (20). The problem is reduced to a two-point boundary-value problem (TPBVP). The authors have developed some efficient solvers for this type of problem by employing fine algorithms such as the steepest ascent method [24], the sequential conjugate gradient-restoration algorithm SCGRA [25,26], and the modified quasi-linearization algorithm MQA [27]. In this paper, the problem is solved by the STP-CODE. The details of the solver are shown in [28]. Although the algorithm is an old one, several techniques such as searching for the solution automatically, avoiding local optima, and accelerating convergence are introduced in this code. In Eq. (35), the first term is to maximize MD with the second missile, while the third term is to maximize MD with the first missile. By appropriately selecting a window function Eq. (34) and penalty function Eq. (33) with their coefficients k_r and k_p, both MDs against two missiles can be maximized, however, the process often tends to maximize one of the MDs and minimize the other. The second term is introduced to prevent this phenomenon. The steps to solve the problem by the code are as follows:

1) Select a nominal aircraft control history to intentionally produce some MDs against both missiles. This can be implemented by taking maximum acceleration toward the right or left side a small distance before the missiles.

2) Calculate the optimal control with a r_{2f} value which is a little larger than the obtained value in the preceding process.

3) If the obtained r_{1f} value (MD against the first missile) is less than the r_{2f} value, then decrease the r_{2f} value, on the other hand, if the obtained r_{1f} value is larger than the r_{2f} value, then increase the r_{2f} value, and recalculate the optimal control. This process usually tends to increase the mean value of the two MDs $r_m = (r_{1f}.r_{2f})^{1/2}$ and is continued until no further improvement of r_m is obtained.

IV. Aircraft Optimal Evasive Patterns in Relation to Relative Geometries with Missiles

Table 1 shows initial conditions and some parameters of vehicles where tail chase geometries are selected. The aircraft parameters employed are those of the YF-16 [29], but the maximum g is set to 7 g, while the YF-16 can produce up to 9 g. The reason is that the aircraft has to compensate for gravitational force, and the practical implementation of a bang-bang type maneuver with maximum acceleration would be difficult. The missile data are those of a typical medium range air-to-air missile.

Before studying two-missile cases, one missile cases are first calculated and the results are shown. The calculations of one missile cases are implemented just by setting the coefficients k_{rf} and k_p in Eq. (35) to be zero. Figure 2 shows the coordinates and initial geometry of the vehicles. The aircraft initial horizontal location is at 2000 m. Figure 3 shows the missile initial horizontal location vs MD. In these cases, the aircraft is assumed to maneuver leftward as a feint

Table 1 Parameters and values

Parameter	Value
Aircraft (military thrust)	
m_a	7500 kg
x_{a0}	2000 m
$C_{L\alpha}$	3.689/rad
$\lvert\alpha_{\max}\rvert$	0.1652
$(a_{a\max})$	7 g
$T_{\max}$	37,894 N
S_a	26 m^2
v_{a0}	290.2 m/s (0.9M)
C_{D0}	0.0224
k	0.260
h_{a0}	4572 m
Missiles (sustainer phase)	
m_{mi0}	176 kg
t_{ei}	8 s
v_{mi0}	644.6 m/s (2.0M)
C_{D0i}	0.90
τ_i	0.5 s
I_{SPi}	250 s
S_{mi}	0.0324 m^2
k_i	0.030
N_{ei}	4
T_{mi}	6000 N
h_{mi0}	4572 m
$C_{L\alpha i}$	35.0/rad
$a_{ci\max}$	30 g

motion at first (Note that maneuvers symmetrical to the x axis produce the same MDs).

The lateral acceleration reduces the velocities of both vehicles, however, the disadvantage of the effect is larger for the aircraft than for the missile, therefore the aircraft gradually increases its lateral acceleration to its maximum value. Next, at a small distance before the missile, the aircraft switches to maximum rightward acceleration to avoid the missile. The following figures show the vehicle trajectories and the aircraft control histories. Figures 4 and 5 show the cases of the initial distance of 2000 and 1000 m, respectively. The CAP time and MD are 5.388 s and 17.25 m, then 2.721 s and 15.74 m, respectively. As a larger initial distance gives the aircraft more room to maneuver, the increased MD is reasonable. As the initial distance decreases to less than 700 m, the MD decreases greatly. Figure 6 shows the case of the initial distance of 400 m, where the aircraft control becomes a bang-bang control and the MD is 6.88 m. Including this bang-bang control, the aircraft maneuvers of this type change the sign of the lateral acceleration once, and are here called type 1.

Figure 7 shows the initial vehicle geometry of two-missile cases. Initial locations of the aircraft and missile 2 are $x_{a0} = 2000$ m, and $x_{m20} = 0$ m respectively. The first missile is located between the

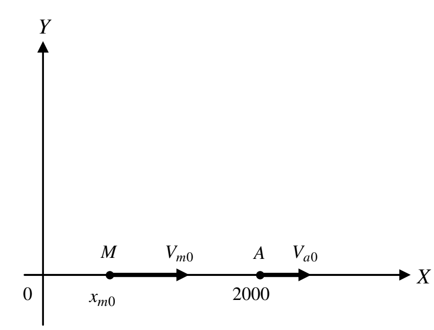

Fig. 2 Vehicle initial geometry and coordinates.

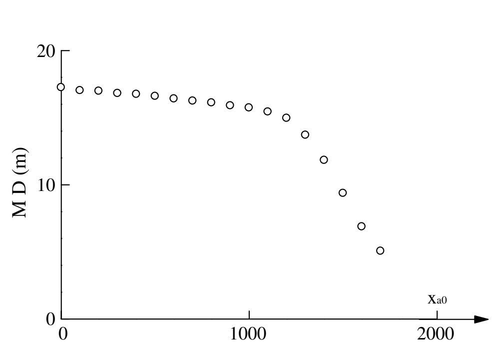

Fig. 3 Missile initial location vs MD.

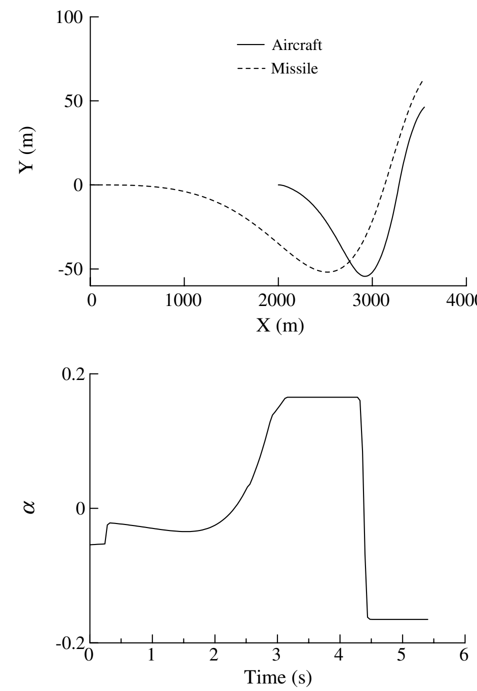

Fig. 4 Vehicle trajectories and aircraft control history (initial distance of 2000 m).

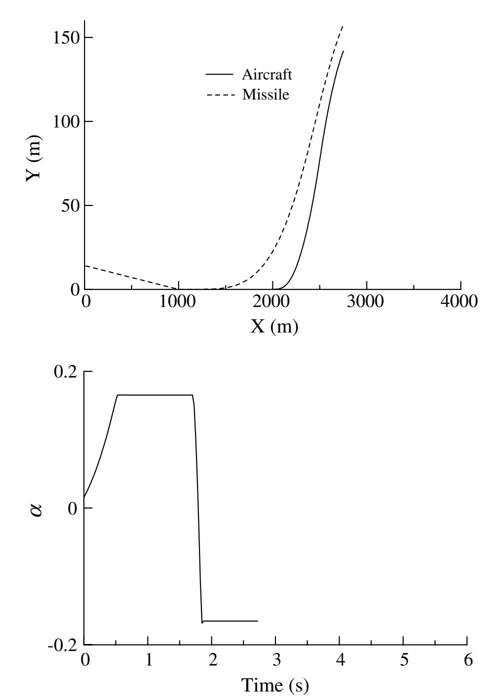

Fig. 5 Vehicle trajectories and aircraft control history (initial distance of 1000 m).

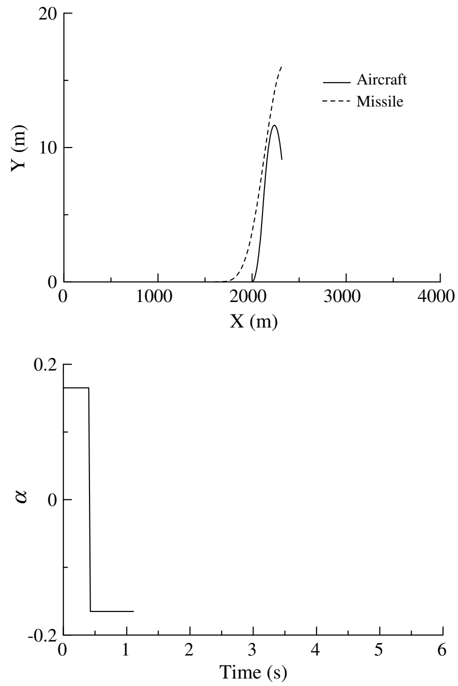

Fig. 6 Vehicle trajectories and aircraft control history (initial distance of 400 m).

aircraft and the second missile, and r_{12} shows the initial distance between missile 1 and missile 2, therefore $r_{12} = x_{m10}$. As symmetrical optimal maneuvers to the x axis exist, the aircraft is assumed to maneuver leftward at first. In this case 3 aircraft evasive patterns appeared. Figure 8 shows the relation between the first missile location and the mean MDs $r_m = (r_{1f} \cdot r_{2f})^{1/2}$ by using the three types of aircraft maneuver. The aircraft avoids the first missile by employing the same maneuver as in the preceding one missile case. Then following this maneuver, if there is enough distance remaining from the second missile, the aircraft can take either of the two types of maneuvers. In the first maneuver, the missile continues to take the maximum rightward acceleration and at a short distance before the second missile, the aircraft switches to maximum leftward acceleration to avoid the second missile. This type of aircraft evasive maneuver changes the sign of the lateral acceleration twice, and is called here type 2. On the other hand, the maneuver to avoid the second missile by maximum rightward acceleration also exists. That is, after avoiding the first missile by using a type 1 maneuver, the aircraft switches again to take the maximum leftward acceleration and at a small distance before the second missile, the aircraft switches to maximum rightward acceleration to avoid the second missile. This type of the maneuver changes the sign of the lateral acceleration three times, and is called here type 3. This type 3 maneuver is more complicated than a type 2 maneuver, and the resultant MD is at most the same value as type 2, therefore a type 2 maneuver is favorable and employed in this section. The advantage of the type 3 is shown in the next section. These type 2 maneuvers generally produce larger MDs than other types, but when the relative distance between the two missiles become very small, the type 1 maneuver becomes effective to avoid two missiles.

The brief summary of this section is that, the aircraft should employ the type 1 maneuvers for r_{12} (the initial distance between two missiles) is less than 300 m, and the type 2 maneuvers for a larger r_{12}, while the missiles can produce the least mean MD r_m at r_{12} is 300 m.

The following figures show the vehicle trajectories and the aircraft control histories for some cases. Figures 9 and 10 show type 2 and type 3 maneuvers for x_{m10} of 1200 m (r_{10} is 800 m). The r_m values for type 2 and type 3 are 13.90 ($r_{1f} = 14.96$ m, $r_{2f} = 12.92$ m) and 13.88 m ($r_{1f} = 14.91$ m, $r_{2f} = 12.91$ m), respectively. Figures 11 and 12 show the vehicle trajectories and the aircraft control histories by using type 1 and type 2 maneuvers for x_{m10} of 300 m (r_{10} is 1700 m). The r_m values for type 1 and type 2 are 13.30 ($r_{1f} = 12.51$ m, $r_{2f} = 14.15$ m) and 13.28 m ($r_{1f} = 14.92$ m, $r_{2f} = 11.82$ m), respectively.

V. Effect of the Missile Trajectory Shaping

If there are two attackers, they can cooperate and launch the missiles from different directions, which will be effective in killing the aircraft. However, in the one-on-one situations of this study, only

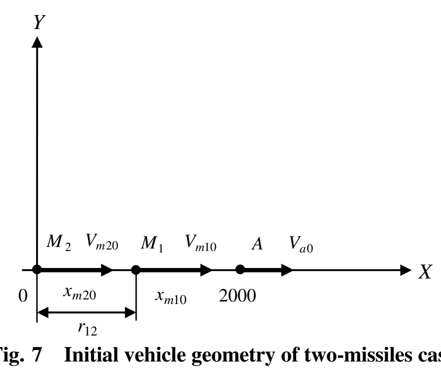

Fig. 7 Initial vehicle geometry of two-missiles case.

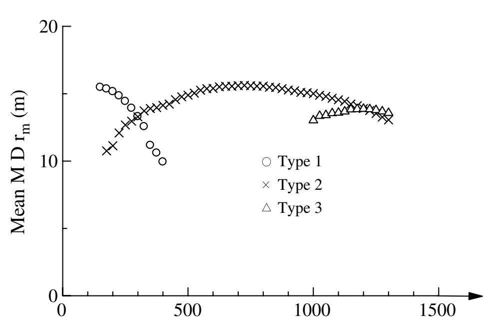

Fig. 8 The first missile location vs the mean MDs by the three types of aircraft maneuver.

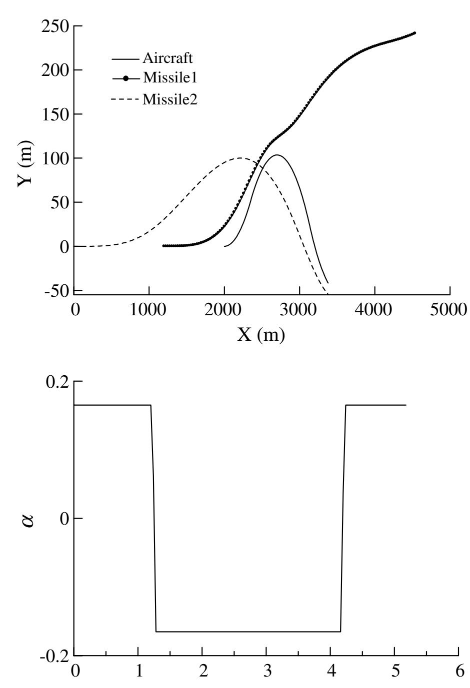

Fig. 9 Vehicle trajectories and aircraft control history with type 2 maneuver for x_{m10} of 1200 m.

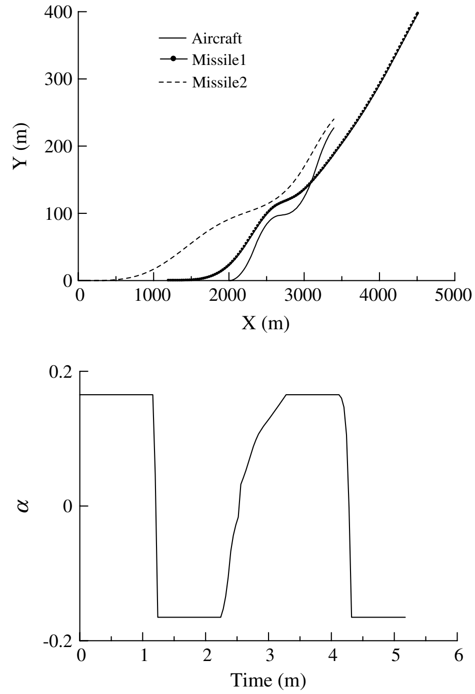

Fig. 10 Vehicle trajectories and aircraft control history with type 3 maneuver for x_{m10} of 1200 m.

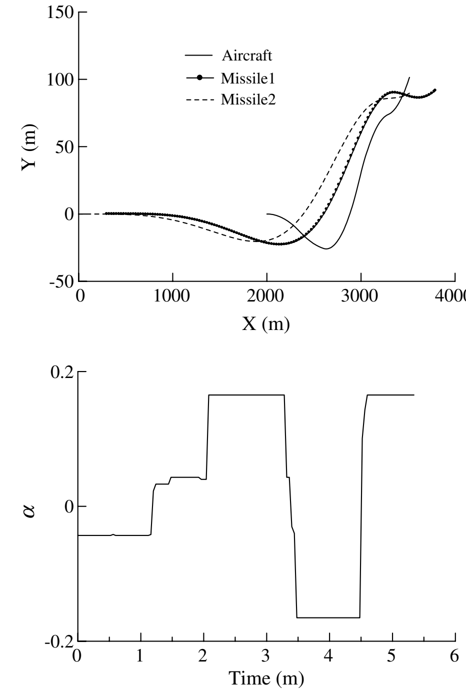

Fig. 12 Vehicle trajectories and aircraft control history with type 2 maneuver for x_{m10} of 300 m.

one attacker can launch two missiles. In this situation the attacker can still distribute the directions of the attacking missiles by employing a trajectory shaping technique. Before this study, the effect of a beam attack was briefly studied. Figure 13 shows the relative geometry between a missile and an aircraft, where their relative distance is 1000 m. The missile initial heading angle ψ_{m0} is on the collision course which is calculated as follows:

Assume the aircraft and the missile velocities v_a and v_m are constant. Let the initial locations of the aircraft and missile be $(x_{a0}, y_{a0}) = (2000, 0)$ and (x_{m0}, y_{m0}) (in meters), and both vehicles are to intercept at t_f at the point P:

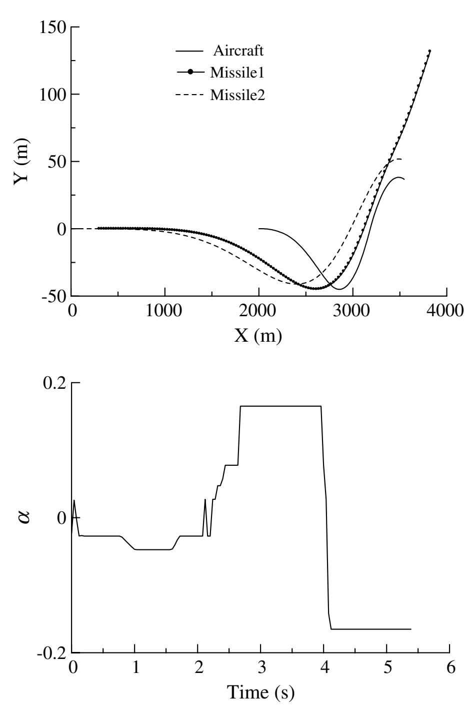

Fig. 11 Vehicle trajectories and aircraft control history with type 1 maneuver for x_{m10} of 300 m.

$$x_{m0} + v_m t_f \cos\psi_m = x_{a0} + v_a t_f$$
$$y_{m0} + v_m t_f \sin\psi_m = y_{a0} = 0 \tag{37}$$

By eliminating t_f from the preceding equations, then

$$(x_{m0} - x_{a0}) v_m \sin\psi_m = (v_m \cos\psi_m - v_a) y_{m0}$$
$$(x_{m0} - y_{a0})^2 v_m^2 (1 - \cos^2\psi_m) = (v_m^2 \cos^2\psi_m - 2 v_a v_m \cos\psi_m + v_a^2) y_{m0}^2$$
$$v_m^2[(x_{m0} - y_{a0})^2 + y_{m0}^2]\cos^2\psi_m - 2 y_{m0}^2 v_a v_m \cos\psi_m + y_{m0}^2 v_a^2 - (x_{m0} - x_{a0})^2 v_m^2 = 0 \tag{38}$$

The preceding equation is solved for $\cos\psi_m$ and ψ_m is obtained. Figure 14 shows the initial σ vs MD by using type 1 maneuvers of the aircraft for the value of σ from -21–$+21$ deg at every 3 deg (x_{m0}, y_{m0}, and ψ_m are determined from the value of σ).

The MD decreases for the value of negative σ, which gives an expectation of the effect of the trajectory shaping of the missiles. Figures 15 and 16 show the vehicle trajectories and the aircraft

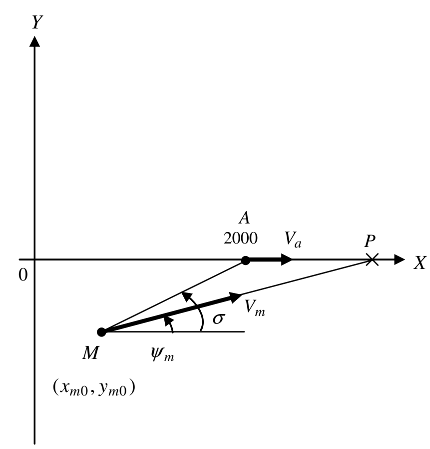

Fig. 13 Relative geometries between a missile and an aircraft.

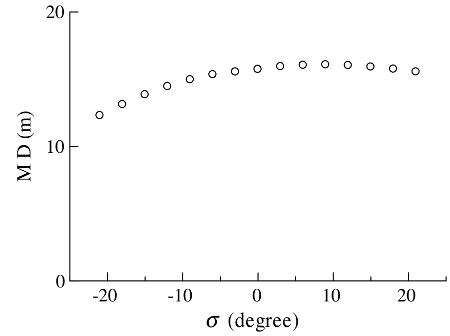

Fig. 14 The initial σ vs MD by using type 1 maneuvers.

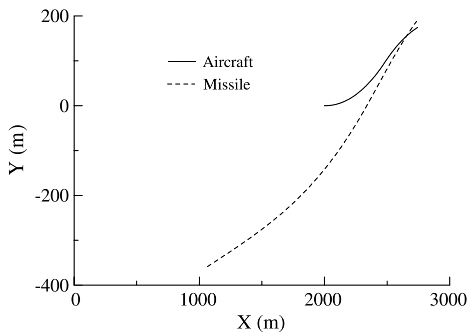

Fig. 15 Vehicle trajectories and aircraft control history for σ is 21.0 deg.

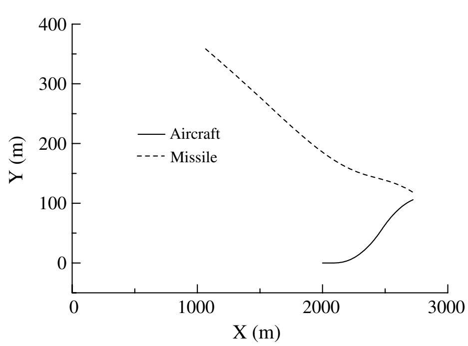

Fig. 16 Vehicle trajectories and aircraft control history for σ is −21.0 deg.

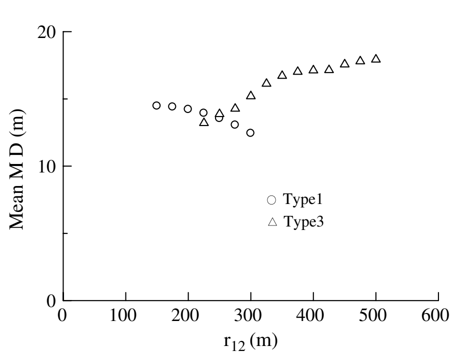

Fig. 17 The mean MD r_m vs r_{12} (the second missile is initially located at the origin).

control histories when the value of σ is 21.0 and −21.0 deg, respectively.

The trajectory shaping of the missiles is implemented by giving bias accelerations to the original acceleration commands by PN in Eq. (29). The study was conducted for several acceleration values and durations in relation to the geometries of two missiles. The cases of applied trajectory shaping to only one missile did not show any reduction of MD (Although it can decrease MD against an aircraft optimal maneuver, it increases MD against the aircraft optimal maneuver symmetrical to the x axis).

Therefore the trajectory shaping was applied to both missiles simultaneously, in a leftward direction for one and a rightward directions for the other. The applied accelerations were 5 g and the durations were 3 s for both missiles. These values were determined by tradeoff studies, that is, a larger acceleration and a duration deteriorate the performance of PN. The study showed that the advantage of using the trajectory shaping appears where the initial

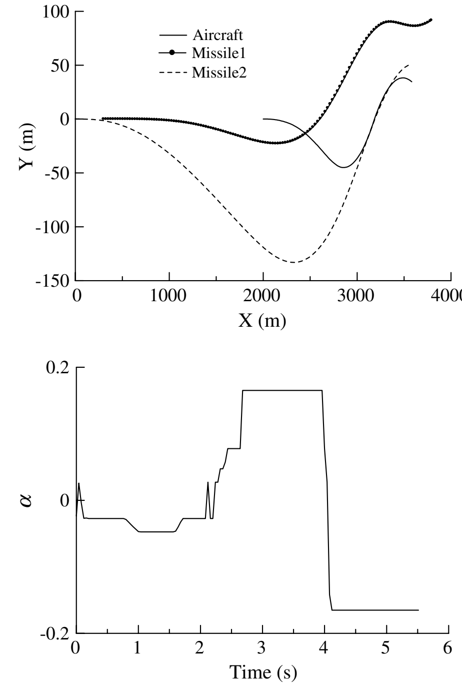

Fig. 18 Vehicle trajectories and aircraft control history by using type 1 maneuver for r_{12} of 250 m (with trajectory shaping).

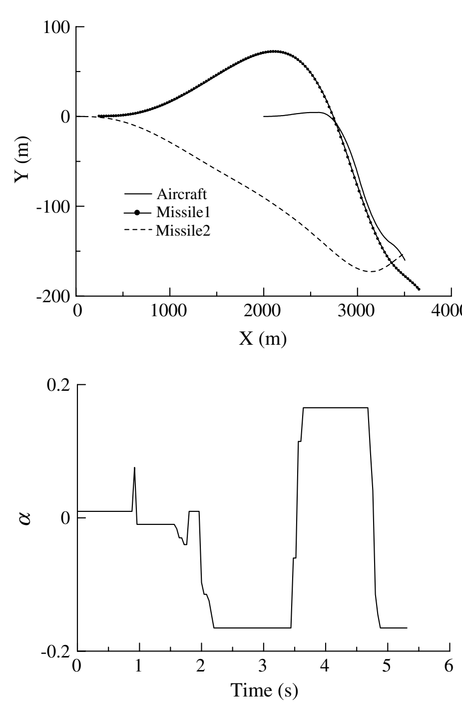

Fig. 19 Vehicle trajectories and aircraft control history by using type 3 maneuver for r_{12} of 250 m (with trajectory shaping).

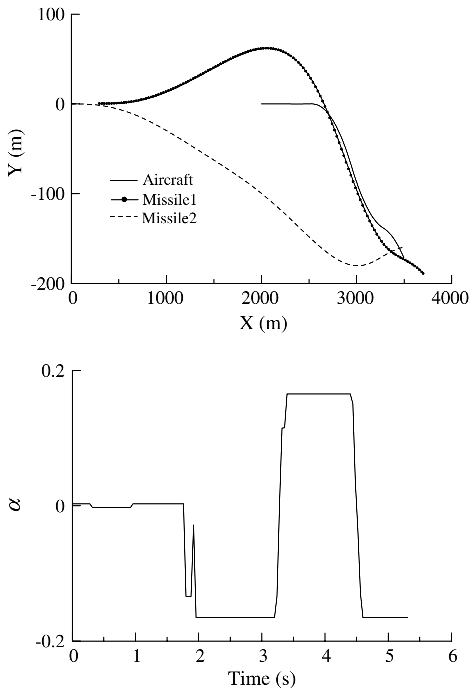

Fig. 20 Vehicle trajectories and aircraft control history by using type 3 maneuver for r_{12} of 300 m (with trajectory shaping).

relative distance between two missiles r_{12} is small. Figure 17 shows the mean MD r_m vs r_{12}, where the second missile is initially located at the origin. Until r_{12} is smaller than 250 m, type 1 maneuvers are employed and the MDs are smaller than the cases in Fig. 8 without trajectory shaping. However if r_{12} is larger than 250 m, type 3 maneuvers are employed and the resultant average MD is larger than with type 2 maneuvers in Fig. 8, without trajectory shaping. Therefore, this study shows that the trajectory shaping should be employed when r_{12} is smaller than 250 m.

Figures 18–20 show the vehicle trajectories and the aircraft control histories by using type 1 and type 3 for r_{12} of 250 m, and then for r_{12} of 300 m using type 3. A sharp protrusion of the aircraft control appears in each of these three figures. It would be impractical to implement these controls, and for practical purposes, they should be approximated by smoother curves. However, as these approximations always caused reduction of MDs, they are shown as they are.

VI. Discussion

The preliminary study showed that if there is not enough time to fly away from the missiles, the aircraft should take the best geometry to the missiles, that is, to take the same line-of-sight angles to both missiles. This geometry is achieved by the aircraft for PN type missiles, including improved PN [30] and augmented PN [1,5,9,22], by taking a heading angle such that the two missiles come to be located on the same line behind the aircraft. The initial geometries of the vehicles are under the assumption that the aircraft has succeeded in taking the geometry. The study against one missile cases in Sec. IV shows that the aircraft has to take an evasive maneuver against the first missile from a distance of at least 700 m before the interception. If there is enough distance remaining after avoiding the first missile, then he can select the type of optimal avoidance from the second missile. In this case, both maneuvers of continuing the maximum rightward acceleration and at an appropriate time switching to the maximum leftward maneuver (type 2), or immediately changing to the maximum leftward maneuver and later switching to the maximum rightward maneuver (type 3) are possible. Therefore in order to kill the aircraft, the distance between two missiles should not be large. However, if the distance is too small, the aircraft can avoid both missiles by an easy type 1 maneuver. In this study, without trajectory shaping of the missiles, the distance of about 300 m is best. The trajectory shaping of the missiles by giving $+5$ and -5 g bias accelerations in addition to PN commands can reduce MDs to some extent where the distance between the missiles is small. In these cases, the distance of about 250 m is best for two missiles. As the trajectory shaping causes a reduction of the missile velocity and gives the aircraft the margin of time and distance, it does not bring in good results unless the distance between the two missiles is small enough. As for the aircraft, against two-missile cases generally speaking type 2 maneuvers are favorable. When the distance between the two missiles is small, type 1 maneuvers are favorable, and if two missiles employ the trajectory shaping stated, type 3 maneuvers are favorable.

In this study, the attacker is assumed to have launched two missiles successively. On the other hand, he may launch the second missile after the first missile has failed. However, in this case the evasive aircraft will employ his afterburner and may fly away from the second missile. This study was conducted based on the data in Table 1. Although the results are not described here, the MDs and the best values of r_{12} decrease for a small value of τ_i, and larger values of $a_{ci\,\max}$ and $a_{a\,\max}$, but the features obtained in this study are the same. Therefore, although recalculation will be required for a specified missile and an aircraft, the results obtained in this study will give valuable information.

VII. Conclusions

The tactics to attack an aircraft with two missiles were studied. The optimal control solver for an aircraft to simultaneously maximize MDs against two missiles was first developed. This was implemented by introducing a special performance index, and by the steepest ascent method. Tail chase geometries between an aircraft and two medium range air-to-air missiles were studied in relation to the mean MD r_m against two missiles. The results showed that there are three types of aircraft optimal evasive maneuvers, which change the sign of the lateral accelerations once, twice, and 3 times, and they are called type 1, type 2, and type 3 maneuvers, respectively. The type 1 maneuver is favorable where the distance between two missiles r_{12} is small. If r_{12} is not small enough, the type 2 maneuver is favorable. The trajectory shaping of the missiles by adding bias accelerations of $+5$ and -5 g in addition to PN commands is effective to some extent, that is, it can reduce r_m against the type 1 maneuvers where r_{12} is small. In this case and if r_{12} is not small enough, the type 3 maneuver is favorable. On the other hand, for the attacker to kill the aircraft with two missiles, the r_{12} should be about 250 m with missile trajectory shaping, and 300 m without it. Although recalculation would be required for specified missiles and aircraft, the feature of the results obtained in this study will give valuable information.

References

[1] Garver, V., "Optimum Intercept Laws for Accelerating Targets," *AIAA Journal*, Vol. 6, No. 11, Nov. 1968, pp. 2196–2198. doi:10.2514/3.4962

[2] Slater, G. L., and Wells, W. R., "Optimal Evasive Tactics Against a Proportional Navigation Missile with Time Delay," *Journal of Spacecraft and Rockets*, Vol. 10, No. 5, May 1973, pp. 309–313. doi:10.2514/3.27759

[3] Shinar, J., Rotsztein, Y., and Bezner, E., "Analysis of Three-Dimensional Optimal Evasion with Linearized Kinematics," *Journal of Guidance, Control, and Dynamics*, Vol. 2, No. 5, Sept.–Oct. 1979, pp. 353–360. doi:10.2514/3.55889

[4] Anderson, G. M., "Comparison of Optimal Control and Differential Game Intercept Missile Guidance Laws," *Journal of Guidance, Control, and Dynamics*, Vol. 4, No. 2, March–April 1981, pp. 109–115. doi:10.2514/3.56061

[5] Nesline, F. W., and Zarchan, P., "A New Look at Classical Versus Modern Homing Guidance," *Journal of Guidance, Control, and Dynamics*, Vol. 4, No. 4, July–Aug. 1981, pp. 78–85. doi:10.2514/3.56054

[6] Imado, F., and Miwa, S., "The Optimal Evasive Maneuver of a Fighter Against Proportional Navigation Missiles," AIAA Paper 83-2139, Aug. 1983.

[7] Forte, I., Steinberg, A., and Shinar, J., "The Effects of Nonlinear Kinematics in Optimal Evasion," *Optimal Control Applications and*

Methods, Vol. 4, No. 2, 1983, pp. 139–152.
doi:10.1002/oca.4660040204

[8] Imado, F., and Miwa, S., "Fighter Evasive Maneuvers Against Proportional Navigation Missile," *Journal of Aircraft*, Vol. 23, No. 11, Nov. 1986, pp. 825–830.
doi:10.2514/3.45388

[9] Imado, F., and Miwa, S., "Fighter Evasive Boundaries Against a Missile," *Computers and Mathematics with Applications*, Vol. 18, Nos. 1–3, Mar. 1989, pp. 1–14.
doi:10.1016/0898-1221(89)90120-X

[10] Ben-Asher, J. Z., and Cliff, E. M., "Optimal Evasion Against a Proportionally Guided Pursuer," *Journal of Guidance, Control, and Dynamics*, Vol. 12, No. 4, July–Aug. 1989, pp. 598–600.
doi:10.2514/3.20450

[11] Imado, F., "Some Aspects of a Realistic Three-Dimensional Pursuit-Evasion Game," *Journal of Guidance, Control, and Dynamics*, Vol. 16, No. 2, March–April 1993, pp. 289–293.
doi:10.2514/3.21002

[12] Imado, F., and Ishiwara, T., "Pursuit-Evasion Geometry Analysis Between Two Missiles," *Computers and Mathematics with Applications*, Vol. 26, No. 6, June 1993, pp. 125–139.
doi:10.1016/0898-1221(93)90122-C

[13] Imado, F., and Miwa, S., "Missile Guidance Algorithm Against High-G Barrel Roll Maneuvers," *Journal of Guidance, Control, and Dynamics*, Vol. 17, No. 1, Jan.–Feb. 1994, pp. 123–128.
doi:10.2514/3.21168

[14] Shinar, J., and Tabak, R., "New Results in Optimal Missile Avoidance," *Journal of Guidance, Control, and Dynamics*, Vol. 17, No. 5, Sept.–Oct. 1994, pp. 897–902.
doi:10.2514/3.21287

[15] Kumar, R. R., Seywald, H., and Cliff, E. M., "Near Optimal Three-Dimensional Air-to-Air Missile Guidance Against Maneuvering Target," *Journal of Guidance, Control, and Dynamics*, Vol. 18, No. 3, May–June 1995, pp. 457–464.
doi:10.2514/3.21409

[16] Ong, S. Y., and Pierson, B. L., "Optimal Planar Evasive Aircraft Maneuvers Against Proportional Navigation Missiles," *Journal of Guidance, Control, and Dynamics*, Vol. 19, No. 6, Nov.–Dec. 1996, pp. 1210–1215.
doi:10.2514/3.21773

[17] Imado, F., and Uehara, S., "High-G Barrel Roll Maneuvers Against Proportional Navigation from Optimal Control Viewpoint," *Journal of Guidance, Control, and Dynamics*, Vol. 21, No. 6, Nov.–Dec. 1998, pp. 876–881.
doi:10.2514/2.4351

[18] Imado, F., and Kuroda, T., "Optimal Aircraft Maneuvers Against Two Proportional Navigation Guided Missiles," *12th International Symposium on Differential Games and Applications* [CD-ROM], Sophia Antpolis, France, July 2006.

[19] Karelahti, J., Virtanen, K., and Ravio, T., "Near Optimal Missile Avoidance Trajectories via Receding Horizon Control," *Journal of Guidance, Control, and Dynamics*, Vol. 30, No. 5, Sept.–Oct. 2007, pp. 1287–1298.
doi:10.2514/1.26024

[20] Karelahti, J., Virtanen, K., and Oestroem, J., "Automated Generation of Realistic Near-Optimal Aircraft Trajectories," *Journal of Guidance, Control, and Dynamics*, Vol. 31, No. 3, May–June 2008, pp. 674–688.
doi:10.2514/1.31159

[21] Garnell, P., "*Guided Weapon Control Systems*," 2nd ed., Pergamon, New York, 1980, Chap. 9.

[22] Zarchan, P., *Tactical and Strategic Missile Guidance*, AIAA, Washington, D.C., 1990, pp. 135–144, 177–183.

[23] Bryson, A. E., Jr., and Ho, Y. C., *Applied Optimal Control*, Wiley, New York, 1969, Chaps. 2, 5, 7, 9.

[24] Bryson, A. E., Jr., and Denham, W. E., "A Steepest Ascent Method for Solving Optimum Programming Problems," *Journal of Applied Mechanics*, Vol. 29, 1962, pp. 247–257.

[25] Wu, A. K., and Miele, A., "A Sequential Conjugate Gradient-Restoration Algorithm for Optimal Control Problems with Non-differential Constraints and General Boundary Conditions, Part 1," *Optimal Control Applications and Methods*, Vol. 1, No. 1, 1980, pp. 69–88.
doi:10.1002/oca.4660010108

[26] Wu, A. K., and Miele, A., "A Sequential Conjugate Gradient-Restoration Algorithm for Optimal Control Problems with Non-differential Constraints and General Boundary Conditions, Part 2," *Optimal Control Applications and Methods*, Vol. 1, No. 2, 1980, pp. 119–130.
doi:10.1002/oca.4660010203

[27] Miele, A., Angiavacchi, A., and Aggarwal, A. K., "Modified Quasilinearization Algorithm for Optimal Control Problems with Nondifferential Constraints," *Journal of Optimization Theory and Applications*, Vol. 14, No. 5, 1974, pp. 529–556.
doi:10.1007/BF00932847

[28] Imado, F., "Pursuit-Evasion Problems of Two Cars in an Ellipsoid Under Gravity," *Engineering Optimization* [online journal], http://www.informaworld.com/smpp/ifirst [retrieved 11 Jan. 2011].
doi:10.1080/0305215x.2010.497184

[29] Gilbert, W. P., Nguyan, L. T., and Gunst, R. W., "Simulator Study of Effectiveness of an Automatic Control System Designed to Improve the High-Angle-of-Attack Characteristics of a Fighter Airplane," NASA TN-8176, May 1976.

[30] Juan, P.-J., and Chen, J.-S., "Ideal Proportional Navigation," *Journal of Guidance, Control, and Dynamics*, Vol. 15, No. 5, Sept.–Oct. 1992, pp. 1161–1165.
doi:10.2514/3.20964